Q. J. R. Meteorol. Soc. (2005), **131**, pp. 1–99 doi: 10.1256/qj.04.n

Mechanisms of ENSO-forcing of hemispherically symmetric precipitation variability

By R. SEAGER[1*], N. HARNIK[1], W. A. ROBINSON[2], Y. KUSHNIR[1], M. TING[1], H.-P. HUANG[1], and J. VELEZ[1]

[1] *Lamont Doherty Earth Observatory of Columbia University, USA*
[2] *University of Illinois at Urbana-Champaign, USA*

Summary

The patterns of precipitation anomalies forced by the El Niño-Southern Oscillation during Northern Hemisphere winter and spring are remarkably hemispherically symmetric and, in the mid-latitudes, have a prominent zonally symmetric component. Observations of global precipitation variability and the moisture budget within atmospheric reanalyses are examined to argue that the zonally symmetric component is caused by interactions between transient eddies and tropically-forced changes in the subtropical jets. During El Niño events the jets strengthen in each hemisphere and shift equatorward. Changes in the subtropical jet influence the transient eddy momentum fluxes and the eddy-driven mean meridional circulation. During El Niño events eddy-driven ascent in the mid-latitudes of each hemisphere is accompanied by low level convergence and brings increased precipitation. This changes in the transient eddy and stationary eddy moisture fluxes almost exactly cancel each other and, in sum, do not contribute to the zonal mean precipitation anomalies. Propagation of anomalous stationary waves disrupts the zonal symmetry. Flow around the deeper Aleutian Low and the eastward extension of the Pacific jet stream supply the moisture for increased precipitation over the eastern North Pacific and the western seaboard of the United States while transient eddy moisture convergence supplies the moisture for increased precipitation over the southern United States. In each case increased precipitation is fundamentally caused by anomalous ascent forced by anomalous heat and vorticity fluxes.

Keywords: ENSO Precipitation Symmetry

1. Introduction

The patterns of off-equatorial precipitation anomalies associated with the El Niño-Southern Oscillation (ENSO) during boreal winter and spring are remarkably hemispherically symmetric. At the Equator, the precipitation anomalies are quite zonally asymmetric with, during El Niño, increased rain in the central and eastern Pacific and reduced rain over the maritime continent, northern South America, the tropical Atlantic and the Indian Ocean. These precipitation anomalies are associated with anomalous diabatic forcing of the global atmosphere circulation. Despite the zonal asymmetry of the diabatic forcing the extratropical response is quite zonally symmetric. During El Niño winters there is increased precipitation across the northern mid-latitudes between about $20°N$ and $60°N$. The largest increase is at the longitude of the East Pacific and the Americas but there is also increased precipitation across Asia. There is also a zonal band of increased precipitation in the Southern Hemisphere centered at about $45°S$.

This pattern is shown in Figure 1a where the precipitation anomalies for the December through May half year, as estimated from the Global Precipitation Climatology Project (GPCP) (Huffman et al. 1997), a blend of satellite and gauge data, are regressed onto the zonal mean zonal wind index of Seager et al. (2003a). The wind index will be described in due course but for now we just need to know that it correlates with the NINO3 SST index (the spatially averaged SST anomaly between $5°S$ and $5°N$ and $150°W$ and $90°W$) at 0.79, indicating that a positive wind index corresponds to El Niño conditions. The wind data are from National Centers for Environmental Prediction-National Center for Atmospheric

* Corresponding author: Lamont Doherty Earth Observatory of Columbia University, Palisades, New York 10964, USA.

Research Reanalysis and the period covered is 1979 to 2001. Figure 1b shows the associated correlation. Some of these elements of ENSO-related precipitation variability were previously noted by Ropelewski and Halpert (1987, 1989, 1996), Kiladis and Diaz (1989) and Aceituno (1988) but here come into better focus because of the use of global satellite data.

The increase in mid-latitude precipitation at most longitudes in each hemisphere during El Niño is statistically significant as seen in Figure 1b. With the brevity of the satellite precipitation record (23 years are used here) correlation coefficients greater than 0.423 are statistically significant at the 95% level. As such the zonally symmetric component of ENSO-related precipitation anomalies appears real and has been remarked on before. Wallace and Jiang (1987) noted that 'the observed wintertime northern hemisphere response to El Niño exhibits a remarkable amount of circular symmetry' which was 'in contrast to the teleconnection patterns' they then discussed, such as the Pacific North America (PNA) pattern (Wallace and Gutzler, 1981). Karoly (1989) stated that, during an El Niño event during southern hemisphere (SH) summer 'there are stable zonally symmetric anomalies of the SH circulation with increased height and temperature at low latitudes and decreased height in middle latitudes'. Seager et al (2003a) have provided an explanation for the zonal symmetry, and mid-latitude cooling during El Niño events, in terms of interactions between transient eddy propagation and the mean meridional circulation. Lau et al. (2004) have provided an alternative explanation in terms of interactions between heating over the Indian Ocean and the Pacific storm track. These studies addressed the atmospheric circulation and temperature response but not the precipitation.

The extensive mid-latitude Northern Hemisphere drought between 1998 and 2002 discussed by Hoerling and Kumar (2003), and which had its Southern Hemisphere counterpart, is related to the ENSO response pattern through the persistent La Niña conditions during this time, even as the anomalous warmth of parts of the Indian Ocean may also play a role. The ENSO response pattern is also very similar to the pattern found in the modeling study of Schubert et al. (2004) to be related to the Dust Bowl drought of the 1930s, a time of persistent but weak La Niña. However drought in the Great Plains, however, are associated with reduced rain during the summer wet season and it remains to be demonstrated how ENSO, which typically peaks during winter, can cause summer rainfall anomalies. The focus here will, however, be on anomalies during northern hemisphere winter and spring.

El Niño related precipitation anomalies around the world can be caused by tropical forcing of large-scale Rossby waves that propagate into higher latitudes (e.g. Horel and Wallace 1981, Hoskins and Karoly 1981, Sardeshmukh and Hoskins 1988, Trenberth et al. 1998, Webster 1981). For example the anomalous Rossby wave train extending north and east from the tropical Pacific during El Niño events causes the North Pacific storm track to extend further east and also to adopt a course further to the south (Trenberth et al. 1998, Wang and Ting 2000). However, a detailed examination of the mechanisms responsible for the related precipitation anomaly has not yet been offered. Furthermore, the causes of the zonally symmetric component remain obscure and probably involve dynamics distinct from Rossby wave teleconnections.

In the current work we seek to explain the physical mechanisms that cause the mid-latitude precipitation variability shown in Figure 1. We will use the National Centers for Environmental Prediction-National Center for Atmospheric Research

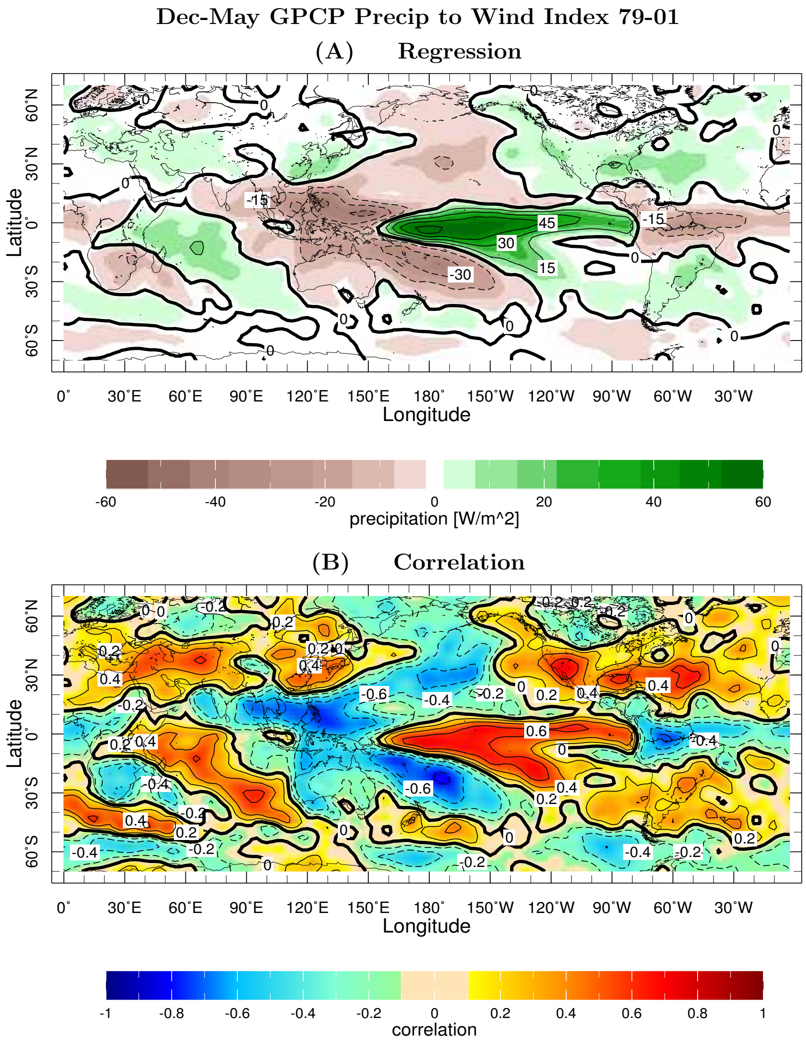

Figure 1. (a) the regression and (b) the correlation of the observed GPCP satellite-gauge precipitation for 1979-2001 with the wind index of Seager et al. (2003) and reflecting El Niño related variability. The units in (a) are Wm^{-2} per standard deviation of the wind index.

(NCEP-NCAR) Reanalysis (Kalnay et al. 1996, Kistler et al. 2001, hereafter 'the Reanalysis') data. There are well publicized errors in the moisture budget of the Reanalysis (Trenberth and Guillemot 1998) and the first part of the paper is devoted to an effort to prove to the reader that, nonetheless, much can be learned about mechanisms of precipitation variability by analyzing the moisture budget in the Reanalysis. We will then evaluate the contributions to ENSO-related global precipitation anomalies from evaporation, stationary and transient eddies, and the zonal mean meridional circulation. Changes in the contribution of these terms to the convergence and divergence of column integrated moisture will then be related to changes in the atmosphere circulation. We will begin by analyzing the zonally symmetric variability and continue by examining regional aspects, in particular the causes of precipitation variability over North America.

It will be claimed that a complete explanation of ENSO forcing of extra-tropical precipitation variability requires interactions between transient eddies and tropically forced changes in the subtropical jets to explain the zonally symmetric component and forced stationary waves, and their interaction with storm tracks, to explain departures from symmetry. Section 2 examines the reliability for our purpose of the NCEP-NCAR Reanalysis, Section 3 briefly reviews the climatological moisture budget, Section 4 examines the zonally symmetric variability, Section 5 examines the regional variability and Section 6 examines how well these patterns are captured in a climate model. Discussion and Conclusions are offered in the final two sections.

2. The usefulness of the NCEP-NCAR Reanalysis for studying mechanisms of interannual precipitation variability

In order to determine the mechanisms of ENSO-forced precipitation variability the various terms in the moisture budget that balance the precipitation - evaporation and convergence of moisture by transient and stationary eddies and by the mean meridional circulation - need to be quantified and related to changes in the atmosphere circulation. This is easy to do with an atmosphere general circulation model (GCM) but sparsity of data makes it hard to do with confidence using observations. Reanalyses, such as the NCEP-NCAR one, appear promising because they provide complete gridded data at high temporal resolution. Reanalysis data consist of observations from various sources, including satellites in the last two decades, that have been assimilated into a weather forecast model. The assimilation procedure fills in the spatial and temporal gaps in the data.

The precipitation field in the Reanalysis is that which the model's parameterizations of moist processes give after the assimilation has been completed. Because the model continually assimilates data and is never run to equilibrium the given precipitation at any place need not balance the sum of the local surface evaporation minus the vertically integrated moisture divergence by the atmospheric flow. The validity of attempts to determine the mechanisms of precipitation variability by examining the different quantities within Reanalysis moisture budget depends on how large this imbalance is.

To examine this question we use three different precipitation estimates. The first is the GPCP satellite-gauge observational data that has already been introduced. The second is the precipitation offered within the NCEP-NCAR Reanalysis. The third was derived from the Reanalysis moisture budget using:

$$P_{der} = E - \frac{L}{gacos\phi}\int_0^{p_s}\left(\frac{\partial\bar{u}\bar{q}}{\partial\lambda} + \frac{\partial(\bar{v}\bar{q}cos\phi)}{\partial\phi} + \frac{\partial\overline{u'q'}}{\partial\lambda} + \frac{\partial(\overline{v'q'}cos\phi)}{\partial\phi}\right)dp. \qquad (1)$$

Here E is the surface latent heat flux, p and p_s are the pressure and surface pressure, u and v are the zonal and meridional velocities along pressure surfaces, q is the specific humidity, L is the latent heat of condensation, g is the gravitational acceleration, a is the radius of the Earth, λ is longitude, ϕ is latitude, overbars denote monthly mean quantities and primes denote departures from the monthly mean. The first two terms within the integral are the divergence of moisture by the monthly mean flow (here containing both the stationary waves and the zonal mean meridional circulation) and the second two are the divergence by transient eddies. P_{der} is here called the NCEP-derived precipitation and is that precipitation implied by the Reanalysis moisture budget. Although both it and E have units of Wm^{-2}, i.e. energy per square meter per second, we refer to them henceforth as simply precipitation and evaporation.

To evaluate P_{der} we used the gridded data and centered differences. Consequently some part of the difference between P_{NCEP} and P_{der} is due to the differences in numerical methods used. However most of the difference between P_{der} and the precipitation given by the Reanalysis, P_{NCEP}, will be because of the imbalance in the Reanalysis moisture budget.

Figure 2 compares the December through May climatological precipitation as given for the period from 1979 to 2001 by the GPCP observational estimates, P_{NCEP} and P_{der}. Clearly the gross structure of the observations is captured by P_{NCEP}, essentially a validation that the model parameterizations of moist processes can produce a reasonable precipitation field when provided with the best estimates of the atmospheric state. In contrast P_{der} contains noticeable errors, especially near steep orography where it can even be negative! Further, there is an excessive noisiness that is obvious despite P_{der} having been smoothed with a 1-2-1 spatial filter. Also values are too high over the dry regions of the subtropical oceans and over tropical continents. Worrisome for our purposes P_{der} has a spurious maximum east of the Rocky Mountains that could occur because too little moisture is rung out of the air as it passes over the model's low-rise representation of the topography.

It is possible that despite the clear errors in the version of the Reanalysis precipitation that is consistent with the moisture budget, the interannual variations may be more faithfully represented. Figure 3 shows the correlation coefficient between the GPCP precipitation for the December through May half year and both P_{NCEP} and P_{der}. P_{NCEP} is highly correlated with the observed precipitation as expected. The correlation with P_{der} is also high in the tropics but declines poleward. Nonetheless P_{der} remains significantly correlated with observations in extensive regions of the mid-latitudes that will be the prime focus here.

The correlations in Figure 3 show how well P_{der} tracks observed precipitation for all forms of variability whereas we are only interested in that which is ENSO-related. In Figure 4 we show the correlation of P_{NCEP} and P_{der} on the wind index. This should be compared with Figure 1b. The associated regression coefficients are shown in Figure 5. P_{NCEP} reproduces the significant correlation of precipitation in the northern hemisphere from the eastern North Pacific across North America to the Atlantic Ocean and also across Asia. It also retains the zonal band of high correlation in the southern mid-latitudes. The precipitation derived from the moisture budget, P_{der}, quite faithfully reproduces the precipitation correlations in the tropics and subtropics, also has the high correlation over the North America sector but basically loses the significant correlation over Asia. Despite being less coherent, a band of significant correlation remains in the southern mid-latitudes. As can be seen in Figure 5, the amplitudes of the P_{der} anomalies are generally reasonable.

Much of the work to be described involves the zonally symmetric signal and in Figure 6 we show the correlation and regression of the zonal means of the GPCP precipitation, P_{NCEP} and P_{der} on the wind index. There is a significant zonal mean precipitation signal with hemispheric symmetry. During an El Niño event it is wet at the Equator, dry in the subtropics and wet in the mid-latitudes of each hemisphere (despite the opposite seasonality). P_{der} captures the observed zonal mean signal with correlation coefficients just as high.

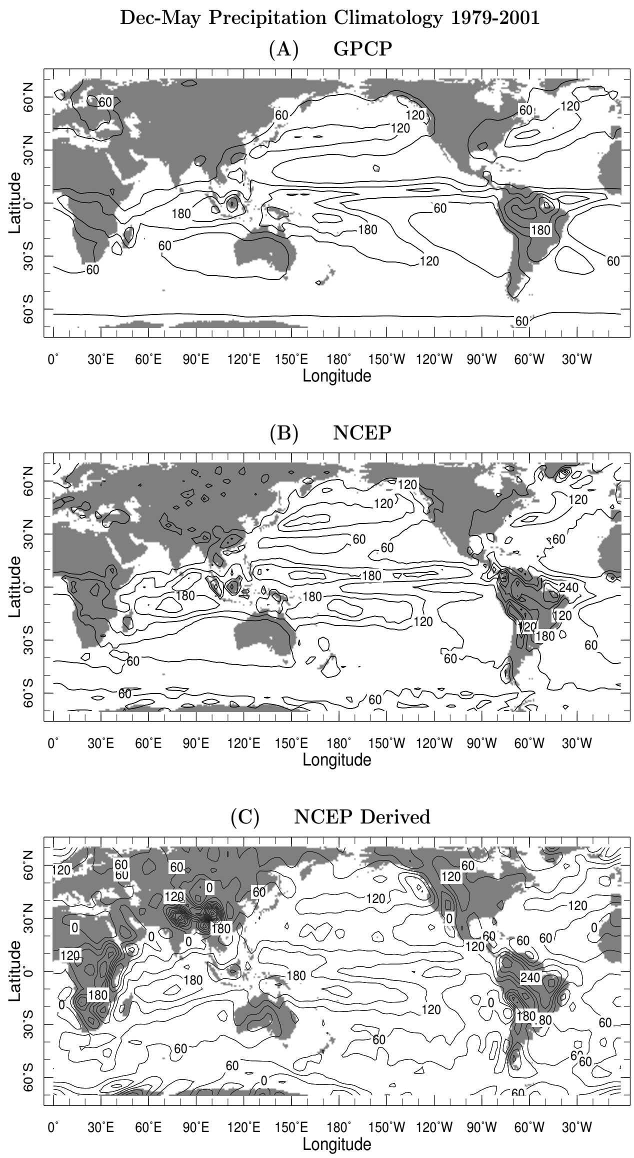

Figure 2. The climatological precipitation for the December through May half year for (a) the GPCP observations, (b) the NCEP precipitation and (c) the derived NCEP precipitation consistent with the NCEP moisture budget. The precipitation has been converted into Wm^{-2}.

On the basis of these intercomparisons a few conclusions can be made. Many aspects of the variations of the NCEP precipitation derived to be consistent with the moisture budget are sufficiently realistic that it makes logical sense to examine the components of the moisture budget that are responsible. This includes the zonal mean, hemispherically symmetric, signal that brings increased precipitation to the mid-latitudes during El Niño. It also includes the increased precipitation from the eastern North Pacific, passing over North America, to the

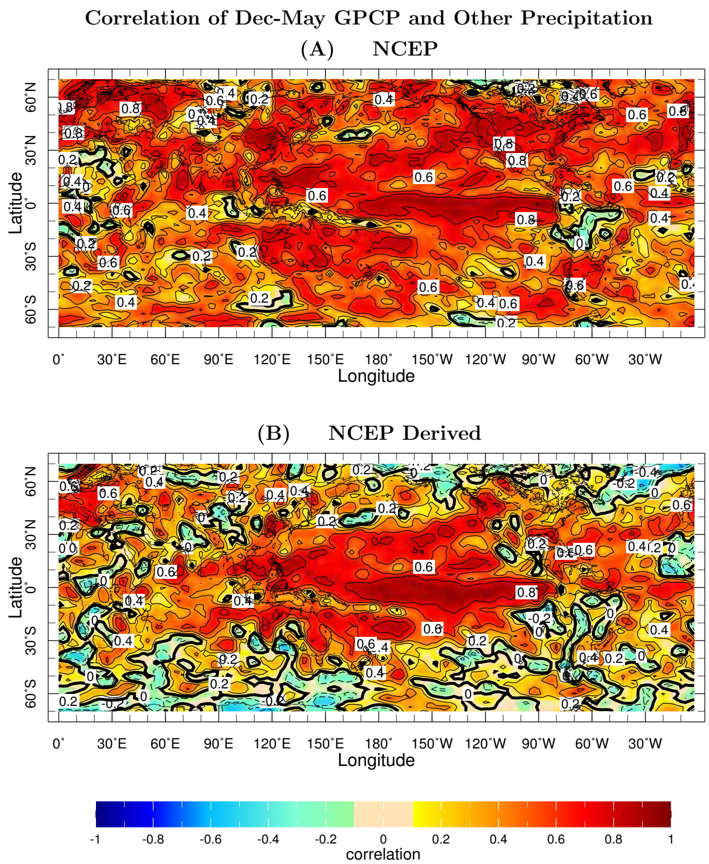

Figure 3. The correlation between the GPCP observed December through May precipitation and (a) the NCEP precipitation and (b) the derived NCEP precipitation consistent with the NCEP moisture budget.

North Atlantic. On the other hand the statistically significant increase in observed precipitation over Asia is not captured in the derived precipitation and there is no point in using the Reanalysis to examine the mechanisms responsible.

3. A brief review of the climatological zonal mean moisture budget

Before examining the nature and causes of extratropical precipitation variability it is worthwhile reviewing those aspcets of the climatological moisture balance which will be useful when considering the interannual variations. More detailed analysis can be found in Peixoto and Oort (1992) and Trenberth and Stepaniak (2003, and references to work by the same authors contained therein). The zonal mean precipitation derived from the moisture budget, $\langle P_{der}\rangle$, is given by the zonal mean of Equation 1:

$$\langle P_{der}\rangle = \langle E\rangle - \frac{L}{gacos\phi}\int_0^{p_s}\left[\frac{\partial}{\partial\phi}\langle\bar{v}\rangle\langle\bar{q}\rangle cos\phi + \frac{\partial}{\partial\phi}\langle\bar{v}^*\bar{q}^*\rangle cos\phi + \frac{\partial}{\partial\phi}\langle\overline{v'q'}\rangle cos\phi\right] dp. \quad (2)$$

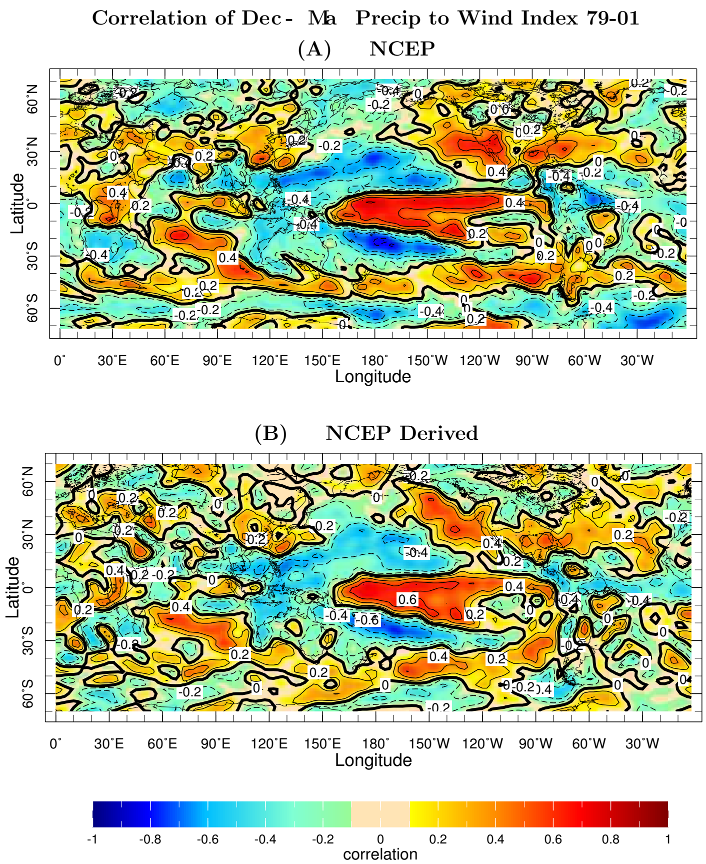

Figure 4. The correlation between the wind index and the December through May precipitation of (a) the NCEP precipitation and (b) the derived NCEP precipitation consistent with the NCEP moisture budget.

In this equation $\langle\rangle$ denotes the zonal mean, * departures from the zonal mean. The first term on the right within the integral is the moisture flux divergence by the mean meridional circulation (MMC), the second is the divergence of moisture by stationary eddies and the third is the divergence of moisture by transient eddies on sub-monthly timescales. The vertical integration is performed using standard discretization techniques from the highest Reanalysis level reporting specific humidity to p_s, thus ignoring Reanalysis levels below ground. The units are Wm^{-2} so although $\langle P\rangle$ and $\langle E\rangle$ are really the associated heat fluxes we refer to them henceforth as precipitation and evaporation.

Each of the terms in Equation 1 was evaluated from the NCEP-NCAR Reanalyses over the period from 1979 to 2001. This period was chosen because of the incorporation of satellite data in 1979 that greatly improves the Southern Hemisphere data coverage.

The balance will be illustrated for the same half year, December through May, for which we examine the variability. Figure 7a compares the latitudinal distributions of $\langle P_{der}\rangle$, $\langle E\rangle$ and the GPCP precipitation. $\langle P_{der}\rangle$ has a double peak in the tropics and smaller peaks in the extratropics of each hemisphere. In

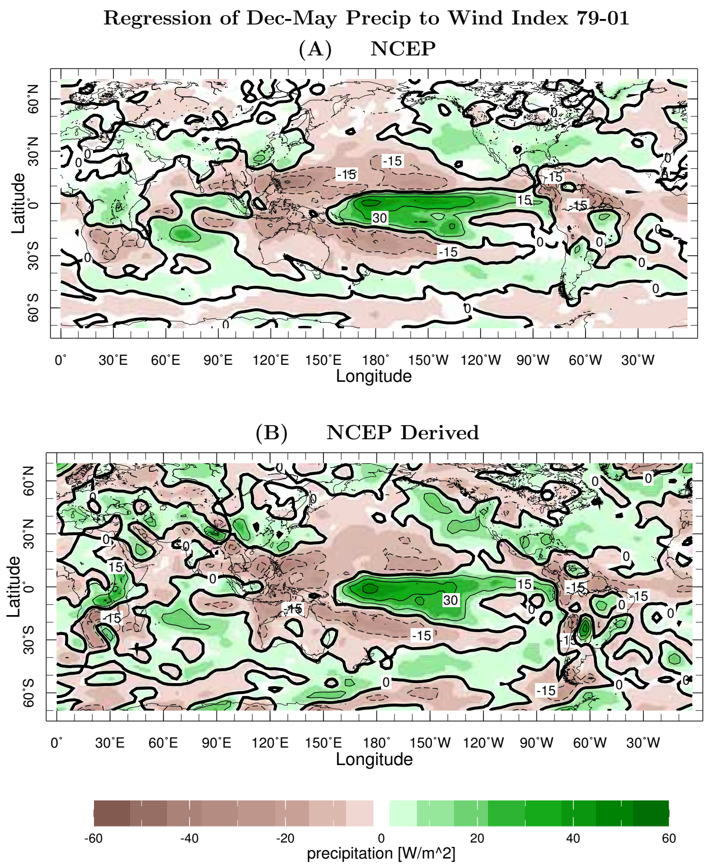

Figure 5. The regression coefficient between the wind index and the December through May precipitation for (a) the NCEP precipitation and (b) the derived NCEP precipitation consistent with the NCEP moisture budget. Units are Wm^{-2} per unit standard deviation of the wind index.

contrast, $\langle E \rangle$ has a minimum at the Equator (Seager et al. 2003b) but otherwise decreases smoothly from the tropics into the mid-latitudes. The extratropical $\langle P_{der} \rangle$ maxima can be largely sustained by the local $\langle E \rangle$ but atmospheric transport of moisture must be responsible for $\langle P_{der} \rangle$ exceeding $\langle E \rangle$ poleward of about $40^\circ N$ and S and for $\langle E \rangle$ exceeding $\langle P_{der} \rangle$ equatorward of there.

Figure 7b shows $\langle P_{der} \rangle$ along with both the convergence of moisture by the mean meridional circulation (MMC) and the convergence by transient eddies. In the tropics the MMC contributes constructively to the $\langle P_{der} \rangle$ distribution. Near the equator rising motion in the convergence zones and monsoons contributes moisture and $\langle P_{der} \rangle$ is in excess of $\langle E \rangle$. In the subtropics descent in the Hadley Cell and subtropical anticyclones contributes drying and $\langle E \rangle$ is in excess of $\langle P_{der} \rangle$. Transient eddies contribute a weak moisture divergence, or drying, within the tropics. In the extratropics both the transient eddies and the MMC - here the Ferrel Cell - converge moisture slightly poleward of the $\langle P_{der} \rangle$ maximum.

Figure 7c shows the stationary eddy moisture flux convergence with, for reference, the transient eddy convergence. The Southern Hemisphere subtropical anticyclones are well developed at this time (Rodwell and Hoskins 2001, Seager

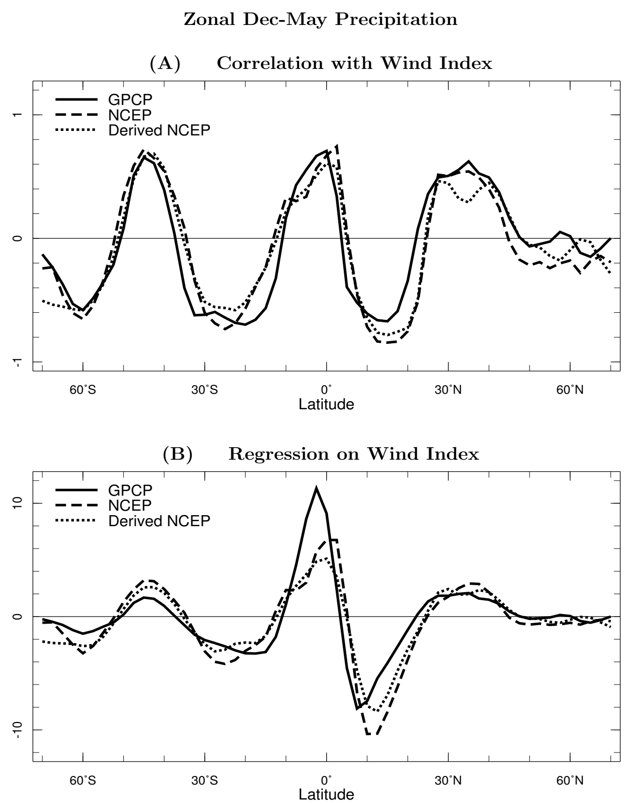

Figure 6. The correlation and regression coefficients between the wind index and the zonal mean December through May precipitation as given by GPCP, the NCEP precipitation and the precipitation derived to be consistent with the NCEP moisture budget. Units for (b) are Wm^{-2} per unit standard deviation of the wind index.

et al. 2003c). Through poleward advection of moist air on their western side and equatorward advection of drier air on their eastern side, the subtropical anticyclones converge moisture between $30°S$ and $40°S$. In the northern hemisphere the equatorward flow in the winter monsoon, extending from West Africa across Asia, of air that is drier than the zonal mean contributes strongly to moisture convergence by the stationary waves at about $25°N$. Poleward of here, moist poleward flow on the eastern flanks of the Aleutian and Icelandic Lows, and dry equatorward flow on the western flanks diverges moisture away from the $30° - 40°N$ latitude band and converges it to the north.

A striking feature is the near complete cancellation of the transient eddy moisture flux divergence around $25° - 40°N$ and S by stationary wave convergence. This allows for the 'seamless' poleward transport of moisture discussed by Trenberth and Stepaniak (2003). The subtropical stationary eddies converge moisture where the atmosphere is statically stable, subsiding and with little precipitation (see Figures 2 and 3 of Seager et al. (2003c). Converging moisture cannot readily be converted into precipitation in such an environment and the transient eddies, which tend to act diffusively on the temperature and humidity distribution, diverge the moisture away. Further poleward in the Northern Hemisphere both the transient eddies and the Aleutian and Icelandic Lows move

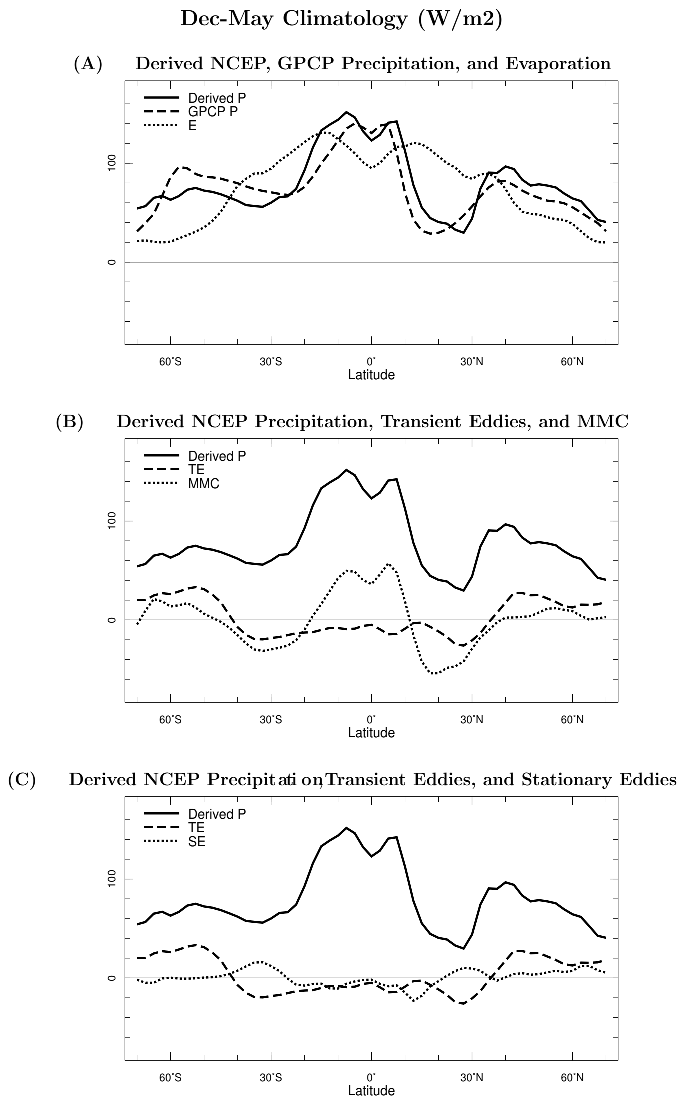

Figure 7. The zonal mean climatological derived precipitation (consistent with the NCEP moisture budget) and terms in the zonal mean moisture budget (see Equation 2) for December through May. The zonal mean derived precipitation is shown in each panel. (a) also shows the GPCP observed precipitation and the zonal mean evaporation, (b) shows the vertical mean convergences of moisture by the transient eddies and the mean meridional circulation and (c) shows the vertical mean convergences of moisture by the transient and stationary eddies. Except for the observed precipitation all data is from the NCEP-NCAR Reanalysis data for the period from 1979 to 2001. Units are in Wm^{-2}

moisture poleward and converge it north of $40°N$. Here there is mean vertical ascent, as can be deduced from the MMC contribution in Figure 7b, and the eddy convergence can be converted into precipitation.

The moisture convergences by the transient eddies and the MMC act constructively in the mid-latitudes. The transient eddy heat and momentum flux convergences both force ascent poleward of about 40° and descent equatorward. Consequently the eddy-driven MMC, forced by each of these processes, has low level moisture convergence poleward of 40° and low level moisture divergence equatorward of there, augmenting the contributions by the transient eddy moisture fluxes. These interrelationships continue to hold for the contributions to the anomalous precipitation.

4. Mechanisms of tropical forcing of zonal mean precipitation variability

(*a*) *Methodology for examination of interannual precipitation variability*

Section 2 demonstrated that the derived precipitation, i.e. that which is consistent with the NCEP moisture budget, captures much of the ENSO-forced extratropical precipitation variability. Therefore, the moisture budget within the Reanalysis can be used to understand the mechanisms responsible. To do this monthly anomalies were computed, using Reanalysis data, of the five terms in the zonal mean moisture budget of Equation 2. December through May anomalies were then formed by averaging monthly anomalies.

All quantities are regressed onto the so-called wind index of Seager et al. (2003a, hereafter S03). It is based on a principal component analysis of the 300mb zonal mean zonal wind performed such that the eigenvectors (Empirical Orthogonal Functions, or EOFs) are in the latitude-calendar month domain with a different time coefficient every year. The first EOF captures variability that is approximately hemispherically symmetric (see S03). The associated time series - the wind index - correlates with the NINO3 SST index (the spatially averaged SST anomaly between $5°S$ and $5°N$ and $150°W$ and $90°W$) at 0.79, indicating that a positive wind index corresponds to El Niño conditions. The PC only has one value per year since the monthly evolution within the year is described by the EOF pattern. Although we could get the same results as presented here by regressing on NINO3 we use the wind index for complete consistency with S03.

(*b*) *Contributions to the zonal mean precipitation variability*

The regressions on the wind index of the terms in the moisture budget are plotted in Figure 8. The precipitation anomalies are not purely accounted for by local evaporation anomalies (Figure 8a). Instead anomalous moisture convergence by the MMC explains most of the zonal structure of the precipitation anomalies (Figures 8b). In the tropics this is because the MMC is the dominant term: as the Hadley Cell intensifies, and the ITCZ moves equatorward from its usual location just north of the Equator, moisture convergence increases at the Equator (where there is anomalous ascent) and decreases in the subtropics (where there is anomalous descent). Outside of the tropics the MMC explains the precipitation anomalies because the transient eddy and stationary eddy convergences, though each individually large, essentially cancel each other. In mid-latitudes the anomalous MMC dries the subtropics and moistens the mid-latitudes, largely because it strengthens during El Niño events (S03). By comparison with the climatological patterns (Figure 7b) it can also be seen that the MMC moisture convergence moves equatorward in both hemispheres causing the mid-latitude precipitation maxima to also shift equatorward during El Niño events.

The extensive cancellation in the subtropics and mid-latitudes between the anomalous moisture flux convergences by the transient and stationary eddies (Figures 8c), allows the continued operation of the 'seamless' total poleward transport (Trenberth and Stepaniak 2003). The transient eddy moisture flux convergence anomaly dries the subtropics and moistens the mid-latitudes while

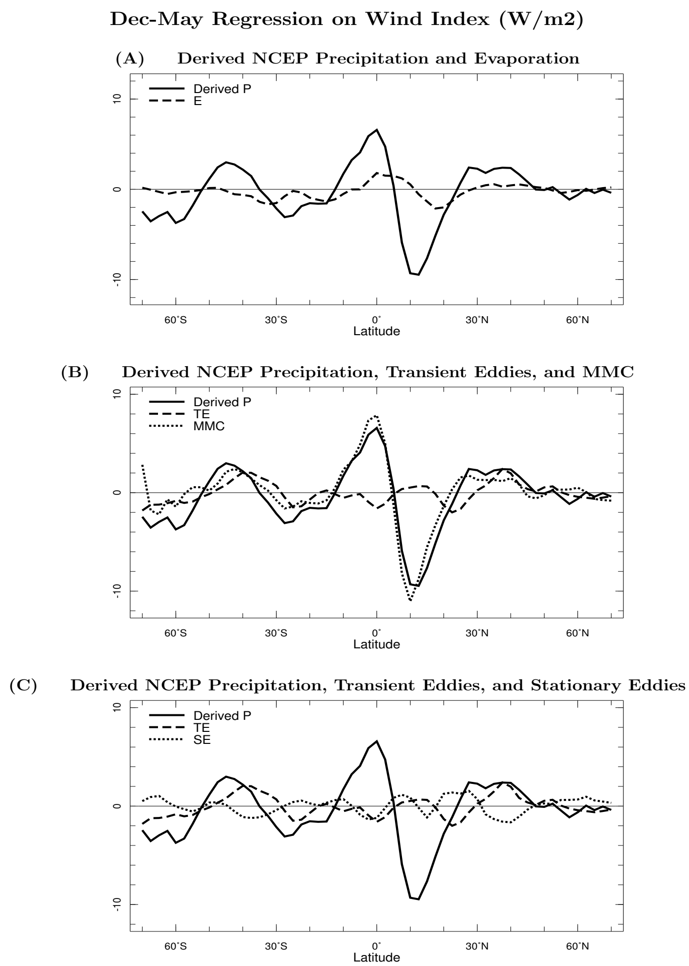

Figure 8. The NCEP-NCAR derived precipitation, and terms in the vertically integrated moisture budget, regressed onto the wind index for December through May. The precipitation is shown in each panel, (a) shows the evaporation, (b) the contributions of moisture convergence by transient eddies and the MMC and (c) the contributions of moisture convergence by transient and stationary eddies. Units are Wm^{-2}

the stationary eddy moisture flux convergence does the opposite. The stationary eddy convergences centered at $25° N$ and S are primarily caused by the anomalous low pressure cells over the Northeast and Southeast Pacific forced by anomalous transient eddy momentum flux convergence (Hoerling and Ting 1994). These lows cause increased equatorward advection of relatively moist air over the central Pacific and increased poleward advection of relatively dry air over the eastern Pacific - an anomalous equatorward moisture transport. The moisture convergences at around $25° N$ and S are compensated by increased transient eddy divergence within the Pacific storm tracks. In both hemisperes, between 30° and 45°, the anomalous moisture divergence caused by the anomalous low pressure cells is cancelled by anomalous transient eddy moisture flux convergence. The stationary wave convergence poleward of $50° N$ is also caused by the stronger than usual Aleutian Low because at this latitude the moistest air is off the coast of British Columbia and Alaska where there is anomalous southerly flow.

(*c*) *Interactions between transient eddies and the MMC and generation of extratropical precipitation variability*

The moisture transport within the MMC best explains increased mid-latitude precipitation during El Niño in both hemispheres. Next we briefly restate the argument of S03 for how the anomalous MMC is caused by an anomalous transient eddy momentum flux that causes eddy-driven ascent (S03).

The all-important element is the strengthening of the subtropical jet streams in each hemisphere. This provides the link between the changes in tropical SST and the changes in the transient eddy fluxes. Using observational analysis and a linear quasi-geostrophic model, S03 show that the stronger subtropical jets during El Niño create regions of anomalously positive meridional gradient of potential vorticity (PV) immediately poleward and anomalously negative gradient further poleward of that. They show that transient eddies, propagating in the latitude-height plane, are refracted away from the region of weaker PV gradient and towards the region of higher gradient, i.e. deeper into the tropics. This creates anomalies in transient eddy momentum flux in the upper troposphere which are balanced by the Coriolis torque associated with anomalous meridional winds. The meridional divergence of these winds drives anomalous ascent in mid-latitudes. S03 show that this ascent causes mid-latitude cooling from the upper troposphere to near the surface in both hemispheres. According to the analysis here, the ascent also causes precipitation.

(*d*) *Transient eddy and stationary wave moisture fluxes and their cancellation*

Associated with the subtropical jet strengthening during El Niño there is an increase in the poleward transient eddy moisture flux (Figure 9a) at the latitudes where the meridional temperature gradient and wind shear (Figure 9b) strengthen (about $30^{\circ}N$ and S). The transient eddy moisture flux decreases further poleward so this is an equatorward shift of the typical pattern†

The latitude-height pattern of the regression on the wind index of $\overline{v'^2}$, a measure of transient eddy activity, shows (Figure 9b) an equatorward shift with prominent areas of increase co-located with the increases in shear and transient eddy moisture flux. This increase in eddy activity is primarily responsible for the increased moisture flux - the increase in the amount of atmospheric moisture is confined too close to the Equator to be available for transport by transient eddies (Figure 9c). Figure 9c also shows the change in the stationary wave flux of moisture and makes clear the degree of cancellation of this with the transient eddy flux. During ENSO cycles the preferred latitudes of the transient and stationary eddies move equatorward and poleward in consort, evidence for a dynamical interplay between the two.

† The increased temperature gradient and wind shear in the subtropics are a result of the tropical heating plus the mid-latitude cooling induced by the transient eddy momentum flux, and subsequent adjustment. In the northern hemisphere the latitude of increased eddy activity and increased eddy moisture transport corresponds to the latitude of the increased subtropical jet and increased vertical shear of the zonal mean zonal wind (Figure 9). In the southern hemisphere, although there are increases in eddy activity and moisture transport at the latitude of the increased subtropical jet, the largest increase occurs poleward where there is a second area of stronger zonal mean zonal wind that extends from the tropopause to the surface. This strengthening bears the hallmarks of being 'eddy-driven' (Lee and Kim 2003) and must arise as part of the eddy-mean flow interactions that cause the cooling of the southern mid-latitudes.

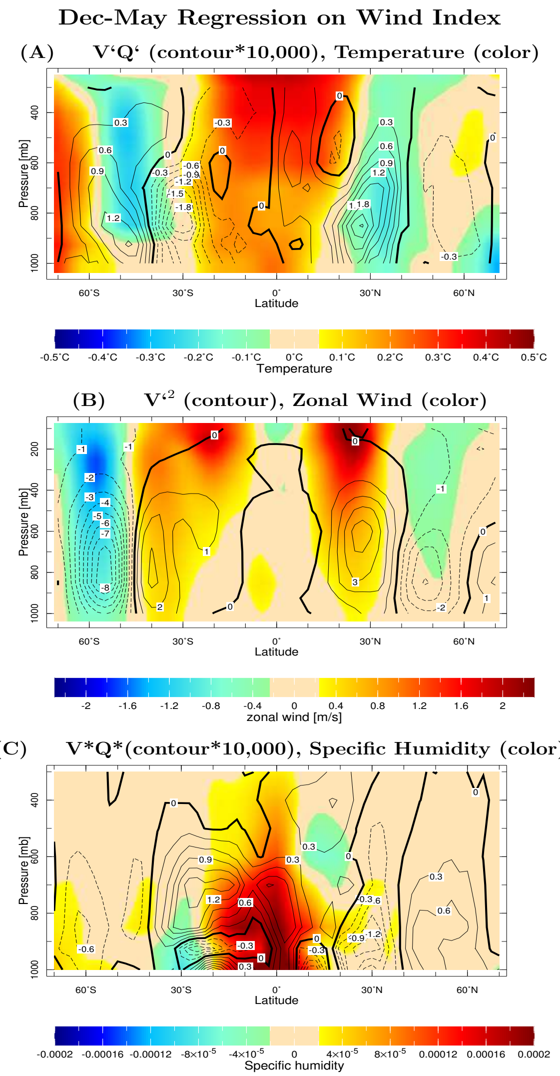

Figure 9. (a) the zonal means of temperature (colors, K) and $\overline{v'q'}$ (contours, ms^{-1} times 10^4), (b) the zonal means of zonal wind (colors, ms^{-1}) and $\overline{v'^2}$ (contours, m^2s^{-2}) and (c) the zonal means of the specific humidity (color) and $\langle\overline{v^*q^*}\rangle$, all regressed onto the wind index, for December through May.

(e) *Summary*

The zonal mean picture is now clear. The subtropical jet strengthening during El Niño impacts the propagation of transient eddies in the upper troposphere, and their associated momentum transports, driving ascent in mid-latitudes that brings increased precipitation. At the same time the patterns of transient and stationary eddy flux convergences shift equatorward relative to their climatological positions with increased transient eddy flux in the subtropics being associated with stronger jets that increase the baroclinicity in the subtropics. However, at all latitudes the transient eddy moisture transports are almost entirely cancelled by the stationary eddy transports. This can be explained by a simple equatorward shift of both the storm track and the stationary eddies during El Niño. Because of this cancellation the precipitation anomalies closely track the moisture convergence by the MMC.

5. Mechanisms of tropical forcing of regional precipitation variability

In addition to the zonally symmetric component of the hemispherically symmetric precipitation variability associated with ENSO, there are important zonal asymmetries. As can be seen in Figure 1 in the northern mid-latitudes the increase in rain during El Niño is greatest in the region stretching from the east Pacific Ocean and over North America to the eastern Atlantic Ocean. In this Section we attempt to explain the regional localization of the tropically forced precipitation variability.

Figure 10 shows the zonal wind at 300mb and $\overline{v'^2}$ at 850mb (corresponding to the level of maximum $\overline{v'q'}$) regressed onto the wind index for December through May. Clearly, during El Niño, the subtropical jets are strengthened the most over the central and east Pacific and over the western North Atlantic. The Pacific strengthening is consistent with the Gill (1980) type response to tropical heating and also with the subtropical part of the Pacific North America (PNA) teleconnection (Wallace and Gutzler 1981, Trenberth et al. 1998). The tropical warming is also maximum in this area (e.g. S03) which could also strengthen the jets locally. The increase in v'^2 on the poleward flank of the northern jet is striking. It is not only in the Pacific but is also clear over the western Atlantic. (This is confirmed in an analysis done using daily Reanalysis data back to 1958 as well as when, for that longer time-period, the data is detrended before the regression to remove any long terms trends.) It represents an eastward extension of the Pacific storm track and a less distinct region of lesser eddy activity between it and the Atlantic storm track. Decrease in v'^2 poleward of the latitudes of increase shows that the anomalies are caused by an equatorward shift in eddy activity.

(*a*) *Analysis of the regional atmospheric moisture budget*

Thinking in terms of the MMC is not useful in explaining regional precipitation anomalies because meridional convergence or divergence is, to first order, balanced not by vertical motion but by zonal divergence or convergence. Instead we determined the contributions of the mean circulation and the transients to the total, zonal plus meridional, convergence of moisture. This involved summing the first two terms and last two terms, respectively, inside the integral in Equation 1, taking anomalies, and regressing on the wind index. The sum of these terms must balance the derived precipitation minus evaporation, $P_{der} - E$. Results are shown in Figure 11.

Looking at the region from the North Pacific Ocean over North America to the North Atlantic Ocean, increased $P_{der} - E$ over the eastern North Pacific and into western North America is sustained by mean flow convergence. This is partly due to flow around the deeper Aleutian Low and partly due to the North Pacific jet extending further east. Northerly flow west of the deeper Aleutian Low reduces $P_{der} - E$ in the central Pacific. The mean flow convergence, associated with stronger westerlies over the western part of the basin (Figure 10a) and general southerly low level flow, also increases $P - E$ over the North Atlantic Ocean.

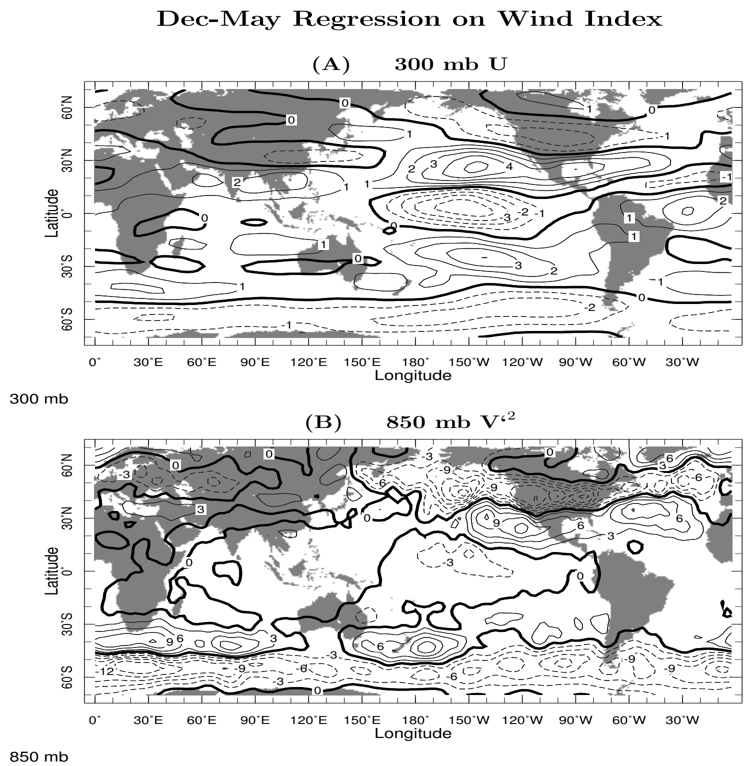

Figure 10. (a) The 300mb zonal wind (colors, ms^{-1}) and (b) the variance of the 850mb meridional velocity, v'^2, (contours, m^2s^{-2}), regressed onto the wind index for December through May.

The transient eddy convergence adds to increased $P_{der} - E$ on the west coast of North America and contributes the increased $P_{der} - E$ in the southeastern United States. In the Southern Hemisphere the mean flow and transient eddy convergences act constructively to provide a band of increased $P_{der} - E$ centered on $40 - 50°S$ that is essentially zonally symmetric.

In both the eastern North Pacific to North Atlantic region, and in the southern mid-latitudes, the moisture flow convergence is larger than the surface evaporation anomalies (Figure 11c). The surface evaporation pattern is also not systematically related to the precipitation pattern. Consequently the patterns of moisture convergence by the atmospheric flow identified can, to first order, be thought of as balancing P_{der} rather than $P_{der} - E$.

(b) *A vertical velocity perspective on extratropical precipitation anomalies in the North American sector*

This analysis identifies the moisture transport anomalies that sustain the precipitation anomalies. However, it is incorrect to think that anomalous moisture convergence, by the mean or transient flow, causes precipitation anomalies. For example, during El Niño events, increased rain in the central tropical Pacific is fundamentally caused by surface ocean warming and an increase in the moist static energy of surface air, which causes convective instability, rather than the increased moisture convergence. In the extratropics it is also possible that increased precipitation is driven by processes that drive increased ascent with the anomalous moisture flux convergence playing a secondary role in stepping

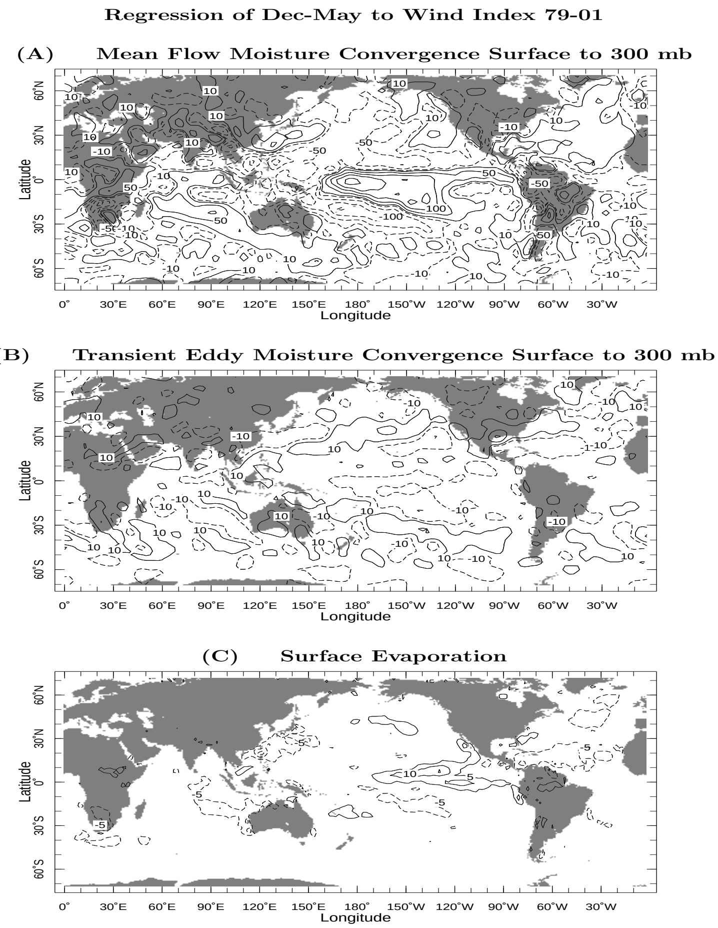

Figure 11. Vertical integrals of the horizontal convergence of moisture by (a) the mean circulation and (b) the transient eddies (ms^{-1} multiplied by 10^6) and (c) the surface evaporation all regressed onto the wind index for December through May. Units are Wm^{-2} per standard deviation of the wind index.

in to supply the moisture required. For example, in the climatology in the subtropics, the transient eddy moisture flux divergence balances the stationary eddy convergence because this is a region of descent and moisture fluxes cannot be converted into precipitation. Similarly, in the zonal mean, the fundamental cause of increased mid-latitude precipitation during El Niño events is the anomalous transient eddy momentum flux that induces ascent. Can we say what induces regional ascent?

The most obvious regionalization of ENSO-related precipitation anomalies in the mid-latitudes occurs in the longitude sector of the Americas, especially around North America. Figure 12a shows the vertical pressure velocity at 700mb regressed onto the wind index for the December through May half year. Comparing to Figure 5b, it is clear that regions of increased precipitation, as estimated by P_{der}, correlate with regions of anomalous ascent with centres west of the United

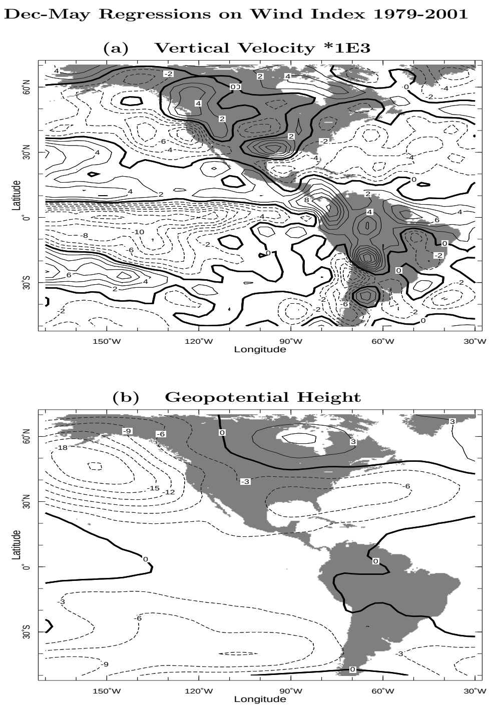

Figure 12. (a) The vertical pressure velocity (Pa per second times 10^3at 700mb) and (b) the 850mb geopotential height (m^2s^{-2}) regressed onto the wind index for December through May.

States and over the subtropical and mid-latitude Atlantic Ocean. A partial explanation for the ascent in these regions is the pattern of the PNA teleconnection: as shown in Figure 12b, during El Niño events there is anomalous low pressure over the eastern North Pacific Ocean and over the North Atlantic Ocean at around $30° - 40°N$. Consequently, there is warm advection immediately west of North America and over the subtropical North Atlantic. Anomalous ascent in these regions occurs partly to balance the advective warming with adiabatic cooling.

However, the match between warm advection and ascent is far from perfect. Ascent over the North Atlantic also occurs to the north of the warm advection and ascent occurs over parts of the eastern North Atlantic where there is anomalous *cold* advection by the mean flow. The mean advective cooling in these areas *is* partially offset by anomalous heat flux convergence but the ascent must be caused by anomalous vorticity fluxes. Indeed, the ascent in these regions is imperfectly related to the anomalies in the advection of mean vorticity by the mean flow in the upper troposphere (not shown). In contrast, the transient eddy vorticity flux convergence bears no systematic relationship to the pattern of local ascent, even as it drives the zonal mean ascent (S03). Further detailed diagnosis of how the temperature and vorticity fluxes combine to cause the observed pattern of ascent and descent is beyond the scope of this paper.

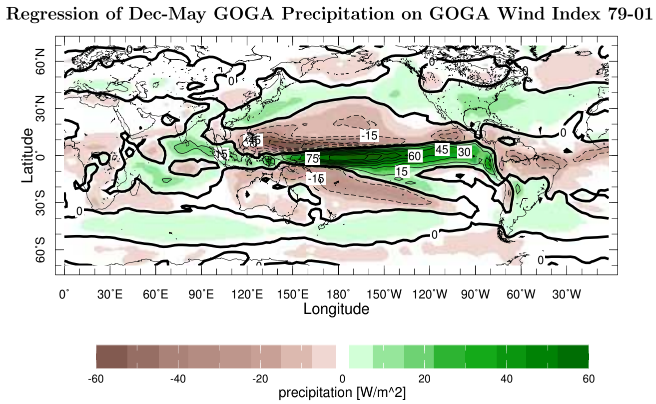

Figure 13. Same as Figure 1 except that the precipitation is taken from the ensemble mean of 16 simulations with the NCAR-CCM3 model forced by observed SSTs. Units are Wm^{-2}.

6. Climate model simulation of tropically forced precipitation variability

ENSO-forced extratropical precipitation variability has significant social consequences as detailed in, for example, Changnon (2000). As such it is worth examining if these patterns can be simulated in climate models. If they can then it should be possible to predict them in advance on the timescale over which tropical Pacific SST anomalies can be predicted.

Here we analyze results from the mean of a 16 member ensemble of simulations conducted at the Lamont Doherty Earth Observatory with the NCAR Community Climate Model 3 (CCM3, Kiehl et al. (1998)) run at T42 resolution with 18 vertical layers. Each ensemble member used observed SSTs (Rayner et al. 2003) in its surface boundary conditions. The 1979 to 2001 period of the simulations was analyzed in a manner identical to the analysis of the Reanalysis.

In Figure 13 we show the model precipitation anomaly, for the December through May half year, associated with the equivalent in the model ensemble mean of the wind index. The wind index, as in observations, describes a hemispherically symmetric variation of the zonal mean zonal winds and correlates with the NINO3 index of the SST field imposed on the model at a higher level than in the Reanalysis. This is no doubt due to the isolation of the boundary-forced variability by taking the ensemble mean. The model precipitation anomaly is similar to that observed. Note the ability of the model to get the increased precipitation in the east Pacific to west Atlantic sector in the Northern Hemisphere, including the maximum in the Southeast United States and the zonally symmetric wet band in the Southern Hemisphere.

There are three differences between model and observations. First, modeled extratropical precipitation anomalies are weaker than observed. Second the modeled variability is more zonally symmetric than the observations, especially in the Southern Hemisphere. This could be because the ensemble mean isolates the boundary-forced component more than can be done in analyzing a mere 22 years of observations or it could be because patterns of precipitation in climate models tend to be more zonally symmetric than in observations. Third the observed

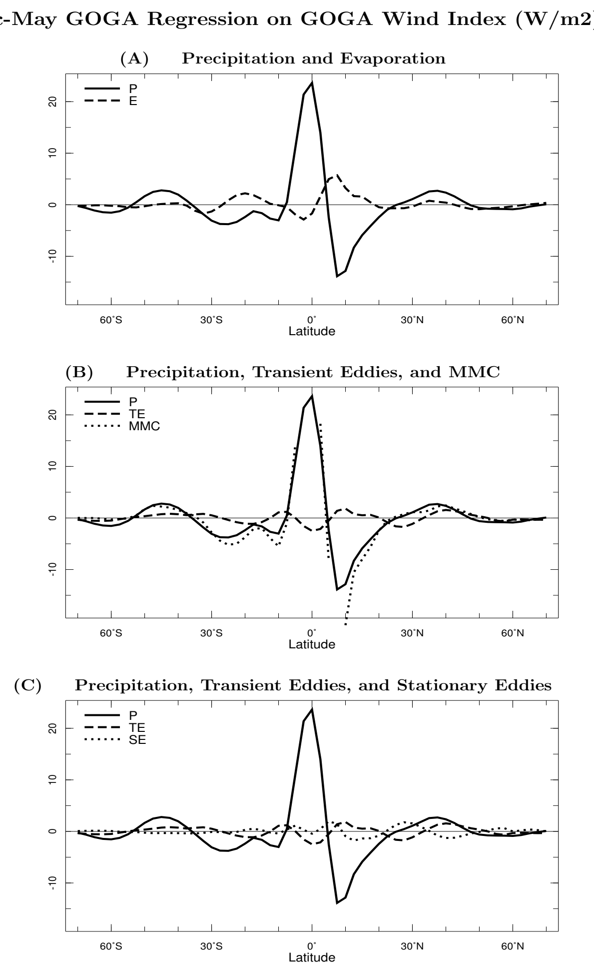

Figure 14. The precipitation, and terms in the vertically integrated moisture budget, regressed onto the wind index for December through May, all quantities taken from the ensemble mean of the 16 simulations with the NCAR CCM3 model. The precipitation is shown in each panel, (a) shows the evaporation, (b) the contributions of moisture convergence by transient eddies and the MMC and (c) the contributions of moisture convergence by transient and stationary eddies. Units are Wm^{-2}

precipitation signal over the Meditterranean and Central Asia is either absent or chronically misplaced in the model.

In Figure 14 we show the mechanisms responsible for the zonal mean precipitation variations in the model. This should be compared to Figure 8. In the model, as in observations, the extratropical precipitation anomalies are primarily induced by the MMC. Also, as in observations, the transient eddy and stationary wave moisture flux convergences cancel each other while each being less potent than observed. The change in transient eddy activity, as measured by $\overline{v'^2}$, is also too weak (not shown) and helps explain why the transient eddy moisture fluxes are too weak. Such errors in could significantly degrade forecasts of ENSO-forced mid-latitude precipitation variability.

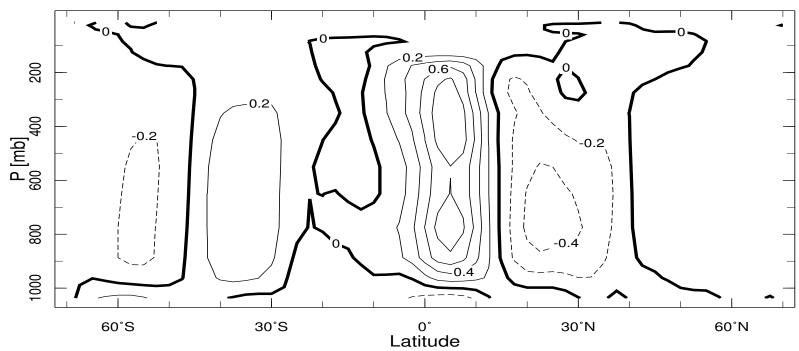

Figure 15. The zonal mean meridional overturning streamfunction regressed onto the wind index for the December through May half year. Units are $10^{10} kg\ s^{-1}$

7. Discussion

(*a*) *The proposed mechanism of tropical forcing of zonally and hemispherically symmetric precipitation variability*

We are now in a position to summarize the proposed mechanism whereby El Niño causes increased zonal mean precipitation during the December through May half year in both hemispheres.

An anomalous surface heat flux from the tropical Pacific Ocean to the atmosphere (Sun 2000) warms the atmosphere immediately above. This warming is rapidly spread throughout the tropical atmosphere as a consequence of equatorial wave propagation and because of the inability of the tropical atmosphere to sustain meridional temperature gradients (Schneider 1977). At the same time increased precipitation causes the Hadley Cell to strengthen (Figure 15). Both processes cause the subtropical jets to strengthen in each hemisphere at the latitude of increased horizontal temperature gradient.

As shown in S03, the changes in the subtropical jet cause perturbations in the meridional gradient of potential vorticity that create a region in the mid-latitudes where transient eddies will adopt a low meridional number. Vertically propagating transient eddies refract away from this area to regions of higher wavenumber, particularly to the upper troposphere of the subtropics. This creates an anomalous poleward flux of zonal eddy momentum in the subtropical upper troposphere. The meridional gradient of the eddy momentum flux has to be balanced by the Coriolis torque operating on the meridional flow creating equatorward flow in the subtropical upper troposphere. By continuity this is balanced by ascent in mid-latitudes. The ascent causes the mid-latitudes to cool (S03) and increases mid-latitude precipitation.

The anomalies in moisture convergence by transient eddies and stationary eddies cancel each other, maintaining their climatological inter-relationship. At the subtropical latitudes of increased vertical shear of the zonal wind and increased meridional temperature gradient (i.e. increased baroclinicity) the transient eddy activity, and transient eddy moisture flux, increase. Both decrease further poleward, reflecting an equatorward shift in the storm tracks. The stationary eddy moisture flux divergence and convergence also shift equatorward cancelling the transient eddy contributions.

(*b*) *Precipitation variability in the North American sector*

In addition to the zonally symmetric variability there are important regional variations. As already well established, El Niño events bring increased precipitation to the eastern North Pacific, the west coast of the United States, across the southern United States and to the western North Atlantic Ocean. This broad band of increased precipitation is sustained by anomalous moisture convergence by the mean flow, in its western portions, and by anomalous transient eddy moisture flux convergence in its eastern portions. However, as for the zonal mean, increased precipitation is more fundamentally caused by anomalous vertical motion and longitudinal variations of this are associated with anomalous stationary waves propagating from the central Pacific. As part of the PNA teleconnection pattern, there is anomalous low pressure over the subtropical and mid-latitude North Pacific and over the subtropical North Atlantic. Warm low level advection on the eastern and southern sides of these anomalous lows forces ascent and increased precipitation. Ascent can also be forced by both vorticity advection by the mean flow and by transient eddy vorticity fluxes. As has been argued, these actually drive the zonal mean ascent and precipitation anomalies and they also certainly influence the regional anomalies but in a complex way. Much future work needs to be done to unravel the tangle of dynamical processes that cause regional precipitation anomalies in mid-latitudes.

(*c*) *Some other relevant ideas on El Niño impacts on transient eddies*

Although the ideas outlined above appear adequate to describe the origins of the observed precipitation anomalies they may not be complete. In particular it has been argued that strengthening of the subtropical jets on their equatorward side alters the life cycles of baroclinic eddies in the region (Thorncroft et al. 1993). Shapiro et al. (2001) applied this argument to the case of the 1997-1999 ENSO to demonstrate that during the El Niño phase baroclinic eddies over the eastern tropical Pacific adopted the Life Cycle 2 of Thorncroft et al. (1993) characterized by longevity and greater waviness. That is broadly consistent with our findings here: the extension of the Pacific stormtrack into the east Pacific and the increased linkage between the Pacific and Atlantic storm tracks is consistent with eddies not decaying in the central Pacific but continuing their life as they propagate further east, while the increased eddy activity, as measured by $\overline{v'^2}$, is consistent with increased waviness. Thus it is quite plausible that the changed eddy behavior over the eastern Pacific-Caribbean-west Atlantic region is not a simple and direct response to increased baroclinicity but also contains the signal of altered baroclinic life cycles. Sorting this out will require considerably more work.

(*d*) *Winter precipitation variability over central and southwest Asia*

Since the 1998 El Niño, Central and southwest Asia has experienced a prolonged drought coincident with persistent La Niña conditions. Barlow et al. (2002) have argued that, not only the La Niña conditions, but also anomalous warmth in the far west Pacific and far east Indian Oceans forced this drought, which was of unusual severity. According to our analysis of the observed precipitation, La Niña conditions alone can produce drought in this area. Since this is not well captured by the precipitation derived to be consistent with the NCEP moisture budget it makes no sense to attempt to determine the mechanisms responsible via the analyses presented here. Nonetheless it is striking that, according to the Reanalysis, La Niña conditions are associated with a weaker subtropical jet across Asia (Figure 10a) and weaker regional baroclinicity (S03) which could, conceivably, cause drying over central Asia, via a local eddy-driven MMC.

(*e*) *Some unresolved issues*

The mechanism for extratropical precipitation variability presented here (and of temperature variability presented in S03) depends crucially on changes in the strength and latitude of the subtropical jets during ENSO. Despite being a well observed and robust feature of the ENSO cycle, first noted by Bjerknes (1966) and identified in atmospheric observations by Arkin (1982), exactly why the jets strengthen (weaken) and move equatorward (poleward) during El Niño (La Niña) remains a matter of mystery.

Three possibilities spring to mind. The first is that it is part of the stationary wave response to the anomalous atmospheric heating in the central tropical Pacific in a manner akin to Gill (1980). This mechanism probably best accounts for why the change in jet strength is most accentuated in the Pacific sector but cannot account for the obvious zonally symmetric component.

Second, the jet change may be a response to the meridional shift of the east Pacific ITCZ. Following the reasoning of Lindzen and Hou (1988), when during El Niño the ITCZ moves southward onto the Equator and convection increases south of the Equator, the Hadley Cell in the Northern Hemisphere should strengthen, as it does (Figure 15), and so should the jet on its poleward flank. However, according to Figure 15, the anomalous Hadley Cell does not extend north enough to reach the anomalous northern subtropical jet and does not strengthen in the southern hemisphere at all (see also Waliser et al. (1999))‡. Locally this argument may work, for example over the central and eastern Pacific where the latitude shift in near equatorial precipitation is most pronounced and where the jets strengthen the most. It cannot explain the hemispherically symmetric component.

The third explanation is that the jets strengthen in response to the anomalous ocean to atmosphere surface heat flux and subsequent tropical warming or cooling. In this case the details of the dynamical adjustment of the atmosphere are unclear but, given that the meridional temperature gradient across the subtropics changes, the jets have to change to maintain thermal wind balance. Because the tropical temperature change has to occur at all longitudes and on both sides of the equator this explanation seems best able to account for both the zonally and hemispherically symmetric components of the subtropical jet anomalies.

In any case, once a change in the subtropical jets has occurred and influenced the transient eddy fluxes of heat and momentum, there will be a subsequent adjustment step in which these altered eddy fluxes impact the jets. The equilibrated state is one that couples together the tropical forcing and the transient eddies.

8. Conclusions

The causes of ENSO-related extratropical precipitation variability have been examined through analysis of the moisture budget contained within the NCEP-NCAR Reanalysis and precipitation estimates provided by the Reanalysis and

‡ The anomalous indirect cells in Figure 14, with rising in the mid-latitudes and sinking in the subtropics, are the signature of the eddy-induced MMC described by S03

satellite data. The period covered was from 1979 through 2001 to match the period of satellite precipitation data and to only include the period in which the Reanalysis assimilates satellite soundings. It was first shown that the ENSO-related precipitation anomalies, as derived from the Reanalysis moisture budget, closely match those in the independent satellite estimates. Thus analysis of the Reanalysis moisture budget to examine the causes of the derived precipitation anomalies has relevance to the mechanisms of the observed precipitation anomalies. We focused on the Northern hemisphere winter and spring seasons because ENSO-related SST anomalies peak at this time as do the related precipitation anomalies.

The principal findings are:

- ENSO-related precipitation anomalies are quite hemispherically symmetric at all longitudes and have a strong zonally symmetric component such that the mid-latitudes of each hemisphere are moist while the subtropics are dry.
- The zonally symmetric component of the precipitation variability is explained in terms of a response to the anomalous heating of the tropical atmosphere during El Niño. This, and the associated strengthening of the Hadley Cell, cause the subtropical jets in each hemisphere to strengthen and move equatorward. As shown in a previous paper (Seager et al. 2003a), the altered subtropical jets tend to steer upward propagating transient eddies away from mid-latitudes and equatorward into the subtropical upper troposphere. This causes eddy-driven ascent in mid-latitudes during El Niño events that induces low level convergence and increased precipitation.
- In the zonal mean the moisture fluxes by the transient and stationary eddies cancel each other such that, in sum, they contribute little to the zonal mean precipitation anomalies. The cancellation occurs as the latitude of transient eddy activity shifts equatorward and the pattern of stationary wave moisture flux convergence and divergence also shifts equatorward.
- Stationary Rossby wave propagation causes important regional departures from symmetry. Over the eastern North Pacific and the western United States increased precipitation during El Niño events is related to eastward extension of the North Pacific subtropical jet stream and southerly flow around a deepened Aleutian Low. Both flow anomalies converge moisture over coastal areas and offshore and can be related to the Pacific-North America teleconnection pattern. Over the southern United States anomalous convergence of moisture by transient eddies provides for increased precipitation and is related to the local strengthening of the subtropical jet and associated baroclinicty. Anomalous ascent is the ultimate cause of the increased precipitation and is related to anomalous warm advection around the low pressure centers of the PNA pattern. Anomalous vorticity fluxes also influence the pattern of anomalous vertical motion.
- In the southern hemisphere the precipitation anomalies are essentially zonally symmetric and accounted for by interactions between the anomalous mean meridional circulation and transient eddies.

Thus there are two dynamically distinct mechanisms of ENSO-related precipitation anomalies in the extratropics. The zonally symmetric component is caused by interactions between the tropically forced mean circulation, the activity and propagation of transient eddies and the eddy-driven mean meridional circulation. The second accounts for important regional deviations from zonal symmetry of precipitation anomalies, such as those over and around North America, and involves the teleconnection, that is, stationary Rossby wave propagation, mechanism.

The division into two mechanisms of extratropical precipitation variability is, to an uncertain extent, a convenient fiction because the zonally symmetric and asymmetric responses will interact. Our main purpose here is to claim that atmosphere dynamics in addition to stationary wave propagation are required for a full explanation of ENSO-related extratropical precipitation anomalies. Recognition of a dynamical mechanism revolving around interactions between transient eddies and the mean meridional circulation provides a framework for explaining why the atmospheric response to ENSO is more zonally symmetric than expected on the basis of stationary wave theory alone (Wallace and Jiang 1987, Karoly 1989). Furthermore, recognition of the degree of zonal and hemispheric symmetry, and a means to explain it, will be useful in interpreting modern and, especially, past records of climate variability and change that appear to contain these characteristics (e.g. Markgraf et al. 2000, Kitzberger et al. 2001, Stine 1994).

Acknowledgements

We would like to thank Naomi Naik and Gus Correa for conducting the climate model simulations. This work was supported by NOAA grants UCSIO-CU-02165401 and NA16GP2024 and NSF grants ATM-9986515 and ATM-9986072. This is Lamont Doherty Earth Observatory Contribution Number xywz.

References

Aceituno, P. 1988 On the functioning of the Southern Oscillation in the South American sctor: Part 1. Surface climate. *Mon. Wea. Rev.*, **116**, 505–524

Arkin, P. 1982 The relationship between interannual variability in the 200mb tropical wind field and the Southern Oscillation. *Mon. Wea. Rev.*, **110**, 1393–1404

Barlow, M., H. Cullen, and B. Lyon: 2002 Drought in central and southwest Asia: La Niña, the warm pool and Indian Ocean precipitation. *J. Climate*, **15**, 697–700

Bjerknes, J. 1966 A possible response of the atmospheric Hadley circulation to equatorial anormalies of ocean temperature. *Tellus*, **18**, 820–29

Changnon, S. A. 2000 *El Niño 1997-1998*. Oxford University Press, New York, 209 pp.

Gill, A. E. 1980 Some simple solutions for heat induced tropical circulation. *Q. J. R. Meteorol. Soc.*, **106**, 447–462

Hoerling, M. P. and A. Kumar 2003 The perfect ocean for drought. *Science*, **299**, 691–694

Hoerling, M. P. and M. Ting 1994 Organization of extratropical transients during El Niño. *J. Climate*, **7**, 745–766

Horel, J. D. and J. M. Wallace 1981 Planetary scale atmospheric phenomena associated with the Southern Oscillation. *Mon. Wea. Rev.*, **109**, 813-829

Hoskins, B. J. and D. J. Karoly 1981 The steady linear response of a spherical atmosphere to thermal and orographic forcing. *J. Atmos. Sci.*, **38**, 1179-1196

Huffman, G. J. et al. 1997 The Global Precipitation Climatology Project (GPCP) Combined Precipitation Dataset. *Bull. Amer. Meteor. Soc.*, **78**, 5–20

Kalnay, E. et al. 1996 The NCEP/NCAR 40-year reanalysis project. *Bull. Am. Meteor. Soc.*, **77**, 437–471

Karoly, D. J. 1989 Southern hemisphere circulation features associated with El Niño-Southern Oscillation events. *J. Climate*, **2**, 1239-1252

Kiehl, J. T., J. J. Hack, G. B. Bonan, B. A. Bovile, D. L. Williamson, and P. J. Rasch 1998 The National Center for Atmospheric Research Community Climate Model: CCM3. *J. Climate*, **11**, 1131–1149

Kiladis, G. N. and H. F. Diaz 1989 Global climatic anomalies associated with extremes in the Southern Oscillation. *J. Climate*, **4**, 1069–1090

Kistler, R. et al. 2001 The NCEP-NCAR 50-year Reanalysis: Monthly means CD-ROM and documentation. *Bull. Am. Meteor. Soc.* , **82**, 247–268

Kitzberger, T., T. W. Swetnam, and T. T. Veblen 2001 Inter-hemispheric synchrony of forest fires and the El Niño-Southern Oscillation. *Glob. Ecol. Biogeog.*, **10**, 315–326

Lau, N.-C., A. Leetmaa and M. J. Nath 2004 Influences of ENSO-induced western Pacific SST anomalies on extratropical atmospheric variability during the boreal summer. *J. Climate*, submitted

Lee, S. and H. K. Kim 2003 The dynamical relationship between subtropical and eddy-driven jets. *J. Atmos. Sci.*,**12**,1490-1503

Lindzen, R. S. and A. Y. Hou 1988 Hadley circulation for zonally averaged heating centered off the Equator. *J. Atmos. Sci.*, **45**, 2417–2427

Markgraf, V., T. R. Baumgartner, J. P. Bradbury, H. F. Diaz, R. B. Dunbar, B. H. Luckman, G. O. Seltzer, T. W. Swetnam, and R. Villalba 2000 Paleoclimate reconstruction along the Pole-Equator-Pole transect of the Americas (PEP 1). *Quat. Sci. Reviews*, **19**, 125–140

Peixoto, J. P. and A. H. Oort 1992 *Physics of Climate*. American Institute of Physics, New York, 520pp

Rayner, N., D. Parker, E. Horton, C. Folland, L. Alexander, D. Rowell, E. Kent, and A. Kaplan 2003 Global analyses of sea surface temperature, sea ice, and night marine air temperature since the late nineteenth century. *J. Geophys. Res.*, **108**, 10.1029/2002JD002670

Rodwell, M. J. and B. J. Hoskins 2001 Subtropical anticyclones and summer monsoons. *J. Climate*, **14**, 3192–3211

Ropelewski, C. F. and M. S. Halpert 1987 Global and regional scale precipitation patterns associated with the El Niño/Southern Oscillation. *Mon. Wea. Rev.*, **114**, 2352–2362

Ropelewski, C. F. and M. S. Halpert 1989 Precipitation patterns associated with the high index phase of the Southern Oscillation. *J. Climate*, **2**, 268–284

Ropelewski, C. F. and M. S. Halpert 1996 Quantifying Southern Oscillation-precipitation relationships. *J. Climate*, **9**, 1043–1059

Sardeshmukh, P. D. and B. J. Hoskins 1988 The generation of global rotational flow by steady idealized tropical divergence. *J. Atmos. Sci.*, **45**, 1228-1251

Schneider, E. K. 1977 Axially symmetric steady-state models of the basic state for instability and climate studies. Part II: non-linear calculations. *J. Atmos. Sci.*, **34**, 280–296

Schubert, S. D., M. J. Suarez, P. J. Region, R. D. Koster, and J. T. Bacmeister 2004 Causes of long-term drought in the United States Great Plains. *J. Climate*, **17**, 485-503

Seager, R., N. Harnik, Y. Kushnir, W. Robinson, and J. Miller 2003a Mechanisms of hemispherically symmetric climate variability. *J. Climate*, **16**, 2960–2978

Seager, R., R. Murtugudde, A. C. Clement, and C. Herweijer 2003b Why is there an evaporation minimum at the Equator? *J. Climate*, **16**, 3792–3801

Seager, R., R. Murtugudde, N. Naik, A. C. Clement, N. Gordon, and J. Miller 2003c Air-sea interaction and the seasonal cycle of the subtropical anticyclones. *J. Climate*, **16**, 1948–1966

Shapiro, M. A., H. Wernli, N. A. Bond, and R. Langland 2001 The influence of the 1997-99 El Niño Southern Oscillation on extratropical baroclinic life cycles over the eastern North Pacific. *Quart. J. Roy. Meteor. Soc.*, **127**, 331–342

Sun, D.-Z. 2000 The heat sources and sinks of the 1986-87 El Niño. *J. Climate*, **13**, 3533–3550

Stine, S. 1994 Extreme and persistent drought in California and Patagonia during mediaeval time. *Nature*, **369**, 546-549

Thorncroft, C. D., B. J. Hoskins, and M. E. McIntyre 1993 Two paradigms of baroclinic-wave life-cycle behaviour. *Quart. J. Roy. Meteor. Soc.*, **119**, 17–55

Trenberth, K. E., G. W. Branstator, D. Karoly, A. Kumar, N. Lau, and C. Ropelewski 1998 Progress during TOGA in understanding and modeling global teleconnections associated with tropical sea surface temperature. *J. Geophys. Res.*, **103**, 14291–14324

Trenberth, K. E. and C. J. Guillemot 1998 Evaluation of the atmospheric moisture and hydrological cycle in the NCEP/NCAR reanalyses. *Clim. Dyn.*,**14**, 213-231.

Trenberth, K. E. and D. P. Stepaniak 2003 Seamless poleward atmospheric energy transports and implications for the Hadley Cell. *J. Climate*,**16**, 3706-3722.

Waliser, D. E., Z. Shi, J. R. Lanzante, and A. H. Oort 1999 The Hadley circulation: assessing NCEP/NCAR reanalysis and sparse in-situ data. *Clim. Dyn.*, 719–735

Wallace, J. M. and Q. Jiang 1987 On the observed structure of interannual variability of the atmosphere/ocean climate system. *Atmospheric and Oceanic Variability*, H. Cattle, Ed., Royal Meteorological Society/American Meteorological Society, 17–43

Wallace, J. M. and D. S. Gutzler 1981 Teleconnections in the geopotential height field during the northern hemisphere winter.*Mon. Wea. Rev.*,**109**,784-812

Wang, H. and M. Ting 2000 Covariabilities of winter U.S. precipitation and Pacific sea surface temperatures. *J. Climate*, **13**, 3711–3719

Webster, P. J. 1981 Mechanisms determining the atmospheric response to sea surface temperature anomalies, *J. Atmos. Sci.*, **38**, 554-571